



Published in final edited form as:

DNA Repair (Amst). 2017 May ; 53: 43–51. doi:10.1016/j.dnarep.2017.02.014.

Probing the Activity of NTHL1 Orthologs by Targeting Conserved Amino Acid Residues[‡]

Susan M. Robey-Bond, Meredith A. Benson[§], Ramiro Barrantes-Reynolds, Jeffrey P. Bond, and Susan S. Wallace^{*}

Department of Microbiology and Molecular Genetics, The Markey Center for Molecular Genetics, University of Vermont, Stafford Hall, 95 Carrigan Drive, Burlington, VT 05405-0068

Abstract

The base excision repair DNA glycosylases, EcoNth and hNTHL1, are homologous, with reported overlapping yet different substrate specificities. The catalytic amino acid residues are known and are identical between the two enzymes although the exact structures of the substrate binding pockets remain to be determined. We sought to explore the sequence basis of substrate differences using a phylogeny-based design of site-directed mutations. Mutations were made for each enzyme in the vicinity of the active site and we examined these variants for glycosylase and lyase activity. Single turnover kinetics were done on a subgroup of these, comparing activity on two lesions, 5,6-dihydrouracil and 5,6-dihydrothymine, with different opposite bases. We report that wild type hNTHL1 and EcoNth are remarkably alike with respect to the specificity of the glycosylase reaction, and although hNTHL1 is a much slower enzyme than EcoNth, the tighter binding of hNTHL1 compensates, resulting in similar k_{cat}/K_d values for both enzymes with each of the substrates tested. For the hNTHL1 variant Gln287Ala, the specificity for substrates positioned opposite G is lost, but not that of substrates positioned opposite A, suggesting a discrimination role for this residue. The EcoNth Thr121 residue influences enzyme binding to DNA, as binding is significantly reduced with the Thr121Ala variant. Finally, we present evidence that hNTHL1 Asp144, unlike the analogous EcoNth residue Asp44, may be involved in resolving the glycosylase transition state.

Keywords

Endonuclease III; base excision repair; enzyme kinetics

[‡]This work was supported by the National Institutes of Health grants R01CA033657 and P01CA098993, awarded by the National Cancer Institute. The automated DNA sequencing and phosphorimaging was performed in the Vermont Cancer Center DNA Analysis Facility and was supported in part by Grant P30CA22435 from the NCI. The views expressed are those of the authors and do not necessarily represent the views of the NIH or NCI.

^{*}To whom correspondence should be addressed. Phone (802) 656-2164. Fax: (802) 656-8749. swallace@uvm.edu.

[§]Current address: Boston Children's Hospital, Harvard Medical School, Department of Medicine, Infectious Diseases Division, 300 Longwood Avenue, Boston MA 02115

Publisher's Disclaimer: This is a PDF file of an unedited manuscript that has been accepted for publication. As a service to our customers we are providing this early version of the manuscript. The manuscript will undergo copyediting, typesetting, and review of the resulting proof before it is published in its final citable form. Please note that during the production process errors may be discovered which could affect the content, and all legal disclaimers that apply to the journal pertain.

Oxidative DNA base damages, estimated to occur about 10,000 times per human cell per day [1], are removed by several overlapping and redundant DNA glycosylases during the process of base excision repair. Base excision repair is initiated when a DNA glycosylase locates the damage and cleaves the N-glycosylic bond, releasing the damaged base. Bifunctional glycosylases also cleave the DNA backbone 3' to the lesion. Other enzymes in the base excision repair pathway then clean the DNA ends, replace the correct nucleotide, and ligate the DNA (for reviews, see [2–8]).

Endonuclease three (Nth) is a bifunctional glycosylase found throughout the phylogenetic tree of life. It removes primarily free radical-damaged pyrimidines, excising lesions with very different chemical structures, which generally do not distort the DNA helix. The mechanisms by which Nth discriminates between normal and damaged bases with different structures are just beginning to be understood [9–11].

The eukaryotic human Nth (hNTHL1) and prokaryotic *Escherichia coli* Nth (EcoNth), while orthologous, have been reported to have important differences in activity. EcoNth and hNTHL1 remove the stereoisomers of thymine glycol (Tg) with a different preference, with hNTHL1 preferring 5R,6S Tg over 5S,6R [12, 13], and EcoNth preferring 5S,6R over 5R,6S [12, 14]. There also appears to be lesion discrimination with regard to opposite base specificity, for example, human NTHL1 prefers the 5R,6S Tg isomer equally well opposite all four bases [13]. However, with both 5-OHC and AP site substrates, human NTHL1 prefers the opposite base guanine [15] while with Tg, it prefers the opposite base adenine [16]. Moreover, in contrast to EcoNth, the lyase activity of human NTHL1 on Tg paired with adenine was 7-times slower than its glycosylase activity [17]; there was no difference when Tg was paired with guanine [16]. In addition, hNTHL1 can remove both lesions from a tandem DHU (under certain conditions), but EcoNth can only remove one [18]. hNTHL1 has been shown to function as a dimer, at least at higher concentrations, via the N-terminal extension (tail) found only in eukaryotic Nth glycosylases [19]. This tail regulates the catalytic turnover of hNTHL1 by substantially reducing the product release in monomers while homodimerization of the tail enhances the rate of product release [19]. EcoNth exists as a monomer.

Using a bioinformatic sequence analysis process that we developed to guide selection as well as examination of the active site of the *Geobacillus stearothermophilus* Nth structure (GstNth) [20], we constructed amino acid variants of hNTHL1 and EcoNth, seeking active site residues that differed between the two enzymes. We then compared binding and catalysis with two chemically similar substrates, 5,6-dihydrouracil (DHU) and 5,6-dihydrothymine (DHT), using single-turnover kinetics. These substrates differ by a methyl group on the pyrimidine ring, and have different cognate bases, C for DHU and T for DHT. Using this approach, we compared substrate recognition and removal between the enzymes, fully excluding the effects of product release. We find, surprisingly, that the glycosylase specificity of the two enzymes is very similar. In addition, Gln287 of hNTHL1 affects substrate recognition, Thr121 of EcoNth is critical for binding and positioning of the substrate, and Asp144 of hNTHL1 plays a different role than its corresponding residue in EcoNth. Thus, the kinetics studies described here have allowed us to further elucidate the basis for the substrate specificity of the Nth enzymes.

Experimental Procedures

Residue selection

Using the PyMol [21] rendering of the GstNth structure (1ORN, [20]) for reference, residues near the active site that differed between hNTHL1 and EcoNth were chosen for analysis (Table 1). The unliganded EcoNth structure [22] superimposes well on the GstNth structure, so it is an appropriate model to use to identify residues at or near the active site. No structure for hNTHL1 is available, but because of the similarity between other human and bacterial HhH-GPD proteins (for example hOGG1 and CacOgg [23], it was assumed that hNTHL1 has a similar active site as GstNth and EcoNth. A method of bioinformatics sequence analysis also guided selection of residues with possible importance to specificity, based on work by Gu [24]. Residue conservation was compared between eukaryotic and prokaryotic clades, noting residues that are conserved in one clade but not the other (residues which have experienced a mutation rate shift), or that are conserved differently between clades (residues that have experienced an amino acid property shift). Two residues with p values slightly greater than 0.05 for property shift were selected to probe for their effect on substrate specificity because of their location near the active site: hNTHL1 Ser140 (EcoNth Ala40) and hNTHL1 Met221 (EcoNth Thr121). The remaining residues chosen for site-directed mutagenesis were culled from the literature [25]. With the exception of hNTHL1Asp144/EcoNthAsp44, all amino acid residues chosen for study differed between hNTHL1 and EcoNth (Table 1).

Enzyme Expression and Purification

The hNTHL1 sequence was cloned as a PreScission Protease cleavable fusion with glutathione-S-transferase into the pGEX-6P-3 expression vector at the *Bam* HI and *Xho* I sites. The resulting purified protein has five amino acids added to the N-terminus: GPLGS, then begins with the hNTHL1 sequence TALSAR. The hNTHL1 enzyme and variants were expressed from the BL21(DE3) *E. coli* strain via auto-induction [26]. From a freshly transformed plate, approximately 20 colonies were used to inoculate 1 L of Terrific Broth (Affymetrix, Inc, Cleveland, Ohio) supplemented with ampicillin and 1X 5052 auto-induction solution (0.5% glycerol, 0.05% glucose, 0.2% α -lactose). The cultures were grown in a 2.8 L Fernbach flask (Fisher Scientific, Hampton, NH) and were shaken at 20° C for approximately 60 h. The cells were harvested and stored at -80° C. To purify the enzyme, the cell pellet was sonicated in lysis buffer (50 mM Tris, pH 8.0, 500 mM NaCl, 5 mM β -mercaptoethanol, 1 mM phenylmethanesulfonyl fluoride) and centrifuged to remove cell debris. The clarified lysate was separated on a glutathione S-transferase (GST) column (GE Healthcare Life Sciences), the peak fractions were collected, and the pooled fractions were dialyzed overnight into protease cleavage buffer (50 mM Tris, pH 8.0, 200 mM NaCl, 5 mM β -mercaptoethanol). PreScission Protease (GE Healthcare Life Sciences) was added (5 U/mg protein) and the protein solution was aliquoted into 1.5 ml centrifuge tubes and gently rocked overnight at 4°C. The aliquots were spun for 10 min in a microcentrifuge to remove precipitate, and the clarified protein solution was run over a GST column again (lysis buffer, except using 200 mM NaCl). This time, the flow-through contained hNTHL1, and was collected. After overnight dialysis into SP buffer (50 mM Tris, pH 8.0, 100 mM NaCl, 10% glycerol, 5 mM β -mercaptoethanol), the sample was run over a HiTrap SP Sepharose

column, eluted with a gradient to 1 M NaCl, and the sample concentrated and dialyzed into storage buffer (50 mM Tris, pH 8.0, 100 mM NaCl, 1 mM DTT, 50% glycerol). EcoNth and variants were expressed and purified as described [27].

Site-directed Mutagenesis

The plasmids harboring wild-type enzyme were used for site-directed mutagenesis using the QuikChange® XL Site-Directed Mutagenesis Kit by Agilent. Primers used to introduce the appropriate variant were designed using the web-based Primer X program (<http://www.bioinformatics.org/primerx/index.htm>).

Substrates

Oligonucleotides (35-mers) were prepared by The Midland Certified Reagent Company, Inc., and were gel-purified, dried as 100 pmol aliquots and stored at -20°C as described [27]. These were reconstituted in 50 μl 10 mM Tris, pH 8.0, and ^{32}P -labeled using T4 polynucleotide kinase. After ethanol precipitation, the radiolabeled substrate was mixed with unlabeled substrate (1:4), annealed with the complement DNA strand (1:1) in 10 mM Tris, pH 8.0, 50 mM NaCl in a 95°C water bath and allowed to cool slowly to room temperature. The sequence was 5'-TGTC AATAGCAAG(damage)GGAGAAGTCAATCGTGAGTCT-3'. The damages used were DHT and DHU, each of which was annealed opposite A or opposite G.

Activity assays

The fraction of enzyme demonstrating activity was determined as previously published [28]. The amount of enzyme added to the glycosylase assays was adjusted for the active fraction; therefore enzyme concentrations are reported as the concentration of active enzyme, not total enzyme.

DNA glycosylase assays

Stock enzyme was diluted with storage buffer to a 10-fold excess of the final reaction concentration. The enzyme was mixed with glycosylase buffer and bovine serum albumin: 2x enzyme, 10 mM Tris, pH 8.0, 1 mM EDTA, 50 mM NaCl, 0.2 mg/ml BSA at room temperature. Substrate was diluted to 2x with glycosylase buffer, and pre-incubated briefly at 37°C . Finally, 16 μl of the enzyme mix was mixed with 16 μl of the substrate mix, and the reaction was stopped at the appropriate time with either 10 μl 1 M NaOH (to measure the glycosylase reaction), or 42 μl formamide (to measure the bifunctional reaction) containing 1 mM EDTA and 0.01% each of xylene cyanol and bromophenol blue. The samples were heated at 95°C for 5 min, formamide solution (32 μl) was added to the samples containing NaOH, and the samples were electrophoresed on a 12% urea gel. The gel was dried, exposed to a phosphorimaging screen, and the density of the substrate and product bands determined using the BioRad Quantity One scanner and software. For wild type EcoNth, the rate of reaction completion necessitated use of a KinTek Rapid Quench RQF-3 apparatus, warmed with a water bath to 37°C . In this case, the reaction was quenched with approximately 200 μl formamide dye solution containing 0.1 M NaOH, freshly prepared. For single turnover

experiments, the experiments were designed to insure that the maximal rate was attained, and that enzyme concentrations chosen bracketed the apparent K_d concentration.

Results

Glycosylase activity of the variants

The variants were constructed to mimic the residue in the orthologous enzyme, in order to determine the residues contributing to the differences between the human and *E. coli* enzymes. For example, hNTHL1 Met221 was mutated to threonine, since the analogous site in EcoNth is Thr121. In the cases where the mutation resulted in an inactive enzyme, the residue of interest was replaced instead by alanine. The variants chosen were screened to determine what effect they might have on substrate specificity.

hNTHL1 cleaves damaged pyrimidines and nicks the DNA backbone but releases the resulting product slowly [29]. In addition, at higher concentrations, the enzyme dimerizes [19], and the dimer stimulates release of the nascent AP site-containing oligonucleotide. Thus for this work, conditions were set so that the glycosylase reaction was examined separately from the bifunctional reaction. The reaction was divided, and the DNA backbone was chemically cleaved with NaOH and heated in order to examine solely the glycosylase reaction; or not treated, in order to examine the bifunctional reaction.

The variant enzymes were screened for substrate specificity compared to wild type under single turnover conditions, with substrate concentrations below known Nth dissociation constants, and enzyme concentrations spanning a range below and above predicted apparent K_d values. Variants that were active yet with different activities than wild type were chosen for further study (italicized in Table 1). Of note, Gln287Arg, Asn279His and Gly280His hNTHL1 variants demonstrated slightly faster glycosylase activity for some substrates than wild type (data not shown); however, no EcoNth variant had greater activity than wild type. The locations of the residues chosen for further kinetic analysis are shown in Figure 1, highlighted on the 1ORN structure of GstNth [20].

Kinetics: model

We used the kinetic model developed by Marenstein et al. [17] to design our experiments (Scheme 1). Because we sought to determine the roles of various amino acid residues in recognizing and removing chemically different substrates, we examined only the kinetics of the glycosylase reaction, not the kinetics of the AP lyase or product release activity of hNTH1 or EcoNth, thus the k_{cat} we measured corresponds to k_2 of the Marenstein model. We chemically resolved the Schiff base by the addition of NaOH to terminate the reaction. Although in our experiments the Schiff base may resolve enzymatically (k_6 and k_7), it is unlikely to contribute to the observed k_{cat} because the reactions were conducted under single turnover conditions. We set the concentration of the substrate less than the expected apparent K_d , and added various amounts of enzyme until the maximal initial reaction rate was observed. The rate constant k_{obs} was determined using the one-phase exponential association equation (first order) $[P] = A_0(1 - e^{-k_{obs}t})$, where A_0 is the amplitude, as described by Porello et al. [30]. Next, the rate constants obtained were plotted against the concentration of

enzyme (using GraphPad Prism software), to obtain a hyperbolic fit, $Y=B_{max} * X / (K_d + X)$, where B_{max} is the fastest rate obtained, and the apparent K_d is the enzyme concentration at half the maximal rate. The apparent K_d and k_{cat} thus obtained were plotted against each other to obtain Figure 2 panels A–H, with 95% confidence intervals shown. The k_{cat} and K_d values are listed in Tables 2 and 3. Because k_{cat} and K_d can co-vary, the specificity of each enzyme for substrate (k_{cat}/K_d) is listed (Table 4).

Wild type enzyme activity

With the exception of DHU:A (Figure 2A, Table 2), the wild type hNTHL1 binds substrates tightly, even more tightly than EcoNth wild type (4–10 times tighter, depending on the substrate). However, the hNTHL1 catalytic rate is much slower than EcoNth, with EcoNth being 3–8 times faster, depending on the substrate, again with the exception of DHU:A (Figure 2E, Table 3).

The enzymes demonstrate a similar pattern of specificity for the substrates, both having greater specificity for substrates opposite G. However, the difference is more pronounced with hNTHL1 (Table 4), thus hNTHL1 demonstrates greater opposite base distinction than EcoNth.

EcoNth cleaves DHT better than hNTHL1

Prior observations in the literature suggest that while EcoNth finds DHT:A to be a poor substrate, it is a relatively good substrate for murine NTHL1 [31]. However, the experimental conditions were such that substrate and enzyme concentrations were well below K_m for EcoNth, but above K_m for mNTHL1, complicating the comparison. We find that the rate of DHT:A base removal is 0.011/s, and 0.085/s for hNTHL1 and EcoNth, respectively, with non-overlapping 95% confidence intervals (Table 2). Therefore, catalytically, DHT is a better substrate for EcoNth than for hNTHL1. Using the measure of specificity k_{cat}/K_d , EcoNth is similarly specific for DHT:A ($0.0006 \text{ nM}^{-1}\text{s}^{-1}$) as is hNTHL1 ($0.0003 \text{ nM}^{-1}\text{s}^{-1}$) (Table 4, Figure 2). Although EcoNth does not bind DHT:A as tightly as does hNTHL1, with an apparent K_d of 137 nM, compared to 31.3 nM for hNTHL1, this result is not statistically significant (Table 3).

DHT is a poorer substrate for both enzymes than DHU

Both hNTHL1 and EcoNth inefficiently catalyze removal of DHT:A. Comparison of k_{cat} values reveals that the rate of removal of DHT is slower than that of DHU (comparing different substrates with like opposite bases: DHU:G vs. DHT:G, DHU:A vs. DHT:A, Table 2). It is also clear, comparing the same substrate with different opposite bases, that catalysis is uniformly slower when A is situated opposite the lesion. Thus, both the lesion DHT and its paired opposite base A contribute to the slower catalysis observed.

hNTHL1 binds to DNA more tightly than EcoNth

Although hNTHL1 catalysis is slower than EcoNth, hNTHL1 binds all substrates tested more tightly than EcoNth, with the exception of DHU:A (Figure 2A and 2E, Table 3). For hNTHL1, the opposite base is a stronger determinant of binding than either substrate tested. This distinction is not observed with EcoNth. Thus, even though hNTHL1 is catalytically

slower, tighter binding is compensatory, with the result that the specificities of hNTHL1 and EcoNth are similar for the substrates tested.

Asp44Val/Asp144Val role shift

The aspartate residue at position 44 in EcoNth is well conserved across phyla. From its position in the structure of GstNth, Asp44 was predicted to promote proton shuttle activity catalyzing β -elimination [20]. In keeping with this prediction, Watanabe et al. [25] found that changing Asp44 to valine in EcoNth (valine is the residue in the analogous position of the monofunctional glycosylase EcoMutY) abrogated lyase activity. We sought to determine whether this residue plays the same role in hNTHL1.

The hNTHL1 Asp144Val variant removes the damaged base 15–230 fold more slowly than wild type hNTH1 (Table 2, Figure 2B). However, the hNTH1 Asp144Val variant binds more tightly to DHT and DHU compared to wild type, and binding of the variant to DHT is tighter than to DHU (Table 3). Because of this tight binding, the specificity (k_{cat}/K_d) (Table 4, Figure 2) of the variant is much higher for DHT compared to DHU, and higher than wild type for all substrates with the exception of DHU:G. The large error bars in Figure 2B reflect that the upper limit for K_d is 0.15 nM, the lowest concentration of substrate we were able to use. However, the best-fit hyperbolic equation predicts the K_d of hNTHL1 Asp144Val for DHT to be 1×10^{-7} nM.

In comparison, the EcoNth Asp44Val variant is also slower than wild type, but to a lesser extent (6–33 fold slower) (Table 2, Figure 2E and F), consistent with observations that Asp44Val allows glycosylase activity but shuts down the lyase function of the enzyme (26). Asp44Val also binds all substrates much more tightly than wild type (40–200 fold). The specificity profile of EcoNth Asp44Val is unchanged compared to wild type (Figure 2), thus it is unlikely that Asp44 plays a role in lesion recognition by EcoNth. Both k_{cat} and K_d trend similarly (Figure 2F). The extremely tight substrate binding of EcoNth Asp44Val, however, plays the contributing role in boosting Asp44Val specificity above that of wild type for all substrates (compare Figures 2E and F). In contrast, the Asp144 of hNTHL1 does not appear to play an important role either in facilitating lesion catalysis or recognizing the opposite base. The k_{cat} of Asp144Val does not vary with lesion type or opposite base (Figure 2B) nor does the opposite base influence binding.

The role of Asp144Val in lesion recognition and removal is further demonstrated by comparing the glycosylase and bifunctional activities of hNTHL1 wild type and hNTHL1 Asp144Val on DHU:G or AP:G (Figure 3). As demonstrated by Watanabe et al [25], the EcoNth Asp44Val lyase activity is severely curtailed, while the glycosylase activity is only slightly affected. Unexpectedly, the hNTHL1 Asp144Val variant impacts glycosylase activity more than lyase activity. The hNTHL1 wild type glycosylase rate was 131-fold faster than the Asp144Val glycosylase rate on DHT:G while the wild type bifunctional rate was only 40-fold faster than the Asp144Val bifunctional rate. Comparing the wild type hNTHL1 glycosylase reaction with the lyase reaction, the glycosylase rate was 12-fold faster than the bifunctional rate, but for Asp144Val, the glycosylase rate was only 3.6-fold faster than the bifunctional rate. Thus, the hNTHL1 glycosylase rate was more severely affected by

replacing Asp144 with valine than was the bifunctional rate, indicating that Asp144 is important for removal of the base lesion in hNTHL1.

EcoNth residue Ser39 has previously been shown to be involved in proton shuttling and when mutated to valine, it loses glycosylase activity [25]. Ser139 is the analogous residue in hNTHL1 and interestingly, when mutated to valine, it also loses glycosylase activity (data not shown).

Arg184Gln/Gln287Ala: role in substrate specificity

In EcoNth, arginine occupies position 184; the corresponding residue in eukaryotes and some archaea is glutamine, and lysine in several other archaea. Thus, an amino acid property shift across clades is observed at this position. As demonstrated by Watanabe and coworkers [25], replacing EcoNth Arg184 with alanine results in a change in substrate specificity. Our work shows a similar effect when glutamine, the residue found at the analogous position in hNTHL1, replaces Arg184. We extended these observations by defining the kinetic parameters of this enzyme variant with the four substrates. In hNTHL1, Gln287Arg was unstable, so we used Gln287Ala.

The hNTHL1 Gln287Ala variant exhibits slower catalysis compared to wild type for all substrates, although similar to wild type hNTHL1, it catalyzes removal of the lesion opposite G faster than opposite A (Figure 2C). Substrates with lesions opposite A are bound more significantly more tightly by Gln287Ala than by the wild type, whereas substrates with lesions opposite G are bound much less tightly by Gln287Ala than by wild type (Table 3). In comparison, wild-type NTHL1 catalyzes of DHU faster than DHT, regardless of the opposite base, and binds substrates opposite G more tightly than opposite A.

Similarly, EcoNth Arg184Gln catalysis is faster for substrates opposite G, and catalysis is slower for all substrates compared to wild type (Figure 2G, Table 3). In contrast to hNTHL1 Gln287Ala, EcoNth Arg184Gln binding is tighter for substrates opposite G, and Arg184Gln loses binding affinity for DHU:A compared to wild type EcoNth.

The specificity profile for hNTHL1 Gln287Ala is very different from wild type hNTHL1 (Figure 3, Table 4). Gln287Ala loses specificity for substrates opposite G, and gains specificity for substrates opposite A. The specificity for DHU:G and DHT:G is similar between the human and the *E. coli* variants, however Gln287A demonstrates much greater specificity for substrates opposite A than does Arg184Gln. The Arg184Gln variant loses specificity for all substrates compared to wild type, mostly due to slower catalysis, but in the case of DHU:A, also due to decreased binding.

Thr121Met/Met221Thr: DNA backbone binding

Residues analogous to position 121 in EcoNth are generally polar (Thr, Ser, Cys) in prokaryotes and hydrophobic (Met, Ile, Val, Leu) in eukaryotes. Both the peptide chain amine and the side chain hydroxyl group of EcoNth Thr121 interact directly with the DNA backbone phosphate 3' to the nucleotide which is 3' to the lesion [20]. In addition, the side chain hydroxyl group hydrogen bonds with a water molecule, which in turn hydrogen bonds with the active site lysine 120 (seen covalently bonded with the open ribonucleoside of the

lesion nucleotide in structure 1ORN, also Figure 1). Thus we would expect that mutation of Thr121 to methionine in EcoNth, would result in the loss of one hydrogen bond to the DNA backbone as well as the interaction in the active site.

When the EcoNth Thr121Met variant was screened for activity, it lost bifunctional activity for DHT:A and DHU:G; however, glycosylase activity was lost only for DHU:G. Because methionine is a bulky residue, and could reduce activity merely due to size, we confirmed the effects with the Thr121Ala variant enzyme. Compared to EcoNth wild type enzyme, Thr121Ala binding to DHU:A was greatly reduced (Figure 2H, Table 3) but the catalytic rate of DHU:A removal was essentially unchanged. However, for DHU:G, the binding was unchanged, and catalysis was greatly reduced. It was not an opposite-base specific effect, however, as Thr121Ala reduced both binding and catalysis for DHT:G and DHT:A. The pattern of substrate specificity was unchanged from wild type (DHU:G>>DHT:G>DHU:A>DHT:A), although specificity fell about 40-fold (Figure 3, Table 4).

hNTHL1 wild type and the Met221Thr variant exhibited similar binding, with the exception of DHT:A (Figure 2D, Table 3). For this substrate, binding is about 16-fold tighter in the variant compared to the wild type protein. This contrasts sharply with the observed binding to DHT:A by hNTHL1 or EcoNth. Both wild type enzymes do not bind DHT:A as well as DHU:G or DHT:G, whereas Met221Thr binds DHT:A similarly to DHU:G and DHT:G. While catalysis of DHU:G and DHT:G is about 1.5 times faster for wild type than the Met221 variant, it is 4–5 times faster in wild type for DHU:A and DHT:A. Thus this variant primarily affects substrate catalysis when the lesion is paired with A.

When we replaced wild type hNTHL1 Met221 with the analogous EcoNth residue Thr, we predicted that hNTHL1 would gain EcoNth character. As expected, the specificity of hNTHL1 Met221Thr for DHT:A increased, and in fact was even better than EcoNth wild type specificity. Since EcoNth Thr121Ala lost significant activity for all substrates, these observations are consistent with EcoNth Thr121 playing an important role in positioning the substrate into the active site. hNTHL1 does not appear to have a counterpart residue.

Discussion

hNTHL1 active site role shift

EcoNth Asp44 participates in lyase activity by mediating resolution of the Schiff base intermediate [20, 25]. We know this because mutation of Asp44 to valine reduces the lyase rate constant to a much greater extent than it reduces the glycosylase rate constant [25]. Mutation of the homologous residue in human NTHL1 Asp144, to valine does not impact lyase activity to as great an extent as in EcoNth but rather it impacts glycosylase activity (Figure 3). Thus, either Asp144 affects glycosylase activity through a different mechanism or it impacts catalysis in some other way, such as through binding. It is parsimonious, then, to conclude that the role of this amino acid changed during evolution of these enzymes from their common ancestor. It appears that, in EcoNth, the glycosylase and lyase reactions are not separable because the glycosylase reaction is the rate-determining step in a two-step reaction, not because the glycosylase and lyase reactions have the same transition state. The

loss of the role for Asp144 in lyase activity is therefore consistent with a reduction in lyase activity and consequent separation of the two roles in the wild type human enzyme.

Opposite base effect

A surprising finding of this work is the role that Gln287 may play in hNTHL1 opposite base recognition. Although the variant Gln287Ala binds substrate opposite G less well, binding to substrates paired opposite A was much tighter (Table 3). The analogous residue in GstNth hydrogen bonds with the 5' phosphate of the lesion, one of several residues that help to position the DNA [20]. However, this binding does not explain the altered opposite base-specific binding. Observation of the structures 1ORN, 1ORP and 1P59 [20] prompts the speculation that this residue may, through a chain of hydrogen bonds, interact with the opposite base. In the 1ORN GstNth structure, a chain of hydrogen bonds exists between the residues Arg185, Asp45, Ser40, Gln42 and the estranged G. The only residue that has direct contact with the opposite base is Gln42, via the carbonyl oxygen, which contacts estranged guanosine at N1 and N2. The analogous residue in hNTHL1 is Gln141. Perhaps an estranged adenosine may interact with the carbonyl oxygen of Gln141 via N1 and N6. If so, the loop from Asp144 to Gln141 would adjust slightly to accommodate these contacts. This adjustment would be prevented by the tighter interactions between Asp144 and Gln287, and interrupted by alanine replacement at that site. This scenario may explain the increased binding of lesions when adenine is the base opposite the lesion upon the replacement of hNTHL1 Gln287 with alanine. Regardless of the opposite base, catalysis by Gln287Ala was impaired, also suggesting a role for this residue in glycosylase activity. This may be via interaction with the neighboring Asp144, as Arg185 and Asp45 are within hydrogen bonding distance in the 1ORN structure. The EcoNth Arg184Gln, a conserved substitution, has largely unaltered binding compared to wild type (with the exception of DHU:A). However, the slower catalysis caused by this substitution is evidence that Arg184 participates in N-glycosylase activity. It could be that the smaller Gln residue may not be properly positioned with Asp44 to facilitate catalysis.

Role of DNA backbone binding by Thr121

The EcoNth Thr121Ala variant decreased binding for three of the four substrates tested (Table 3), experimentally confirming that Thr121 is important in DNA binding [20]. Additionally, the substitution of alanine for threonine impacted catalysis, again for three of the four substrates tested (Table 2), supporting the structural evidence that Thr121 stabilizes Lys120 via a bridging water [20]. It was interesting that the variant affected only binding to DHU:A and only catalysis for DHU:G, but impacted both binding and catalysis for DHT:G and DHT:A.

hNTHL1 Met221Thr only affects binding when the substrate is DHT:A (Table 3), in this case increasing the binding. Taken together with the EcoNth Thr121Ala data, the role of threonine adjacent to the catalytic lysine is to position DNA, but this positioning appears to be dependent on the nature of the substrate. The smaller substrate, DHU opposite G, is accommodated in the binding pocket more easily, but the bulkier substrate, DHT, and substrates opposite A, require proper positioning for catalysis, which Met221Thr or Thr121 provide.

EcoNth and hNTHL1 demonstrate similar substrate specificity for DHT

The N-terminus of hNTHL1 is involved in the dissociation of enzyme and product [29]. Since EcoNth does not have the extended N-terminus, we sought to avoid this mechanistic step when comparing the activities of EcoNth and hNTHL1, hence the limitation of this work to single turnover kinetics. Earlier kinetic experiments with hNTHL1 also attempted to avoid the product dissociation step, but did not definitively establish single-turnover conditions [12, 31]. These workers note that the k_{cat} is independent of lesion for mNTHL1 [31], which we did not observe for hNTHL1. Given that the lyase reaction is rate limiting for hNTHL1, and has a common intermediate regardless of the initial substrate, it is likely that the prior work examined the rate-limiting lyase reaction. We used concentrations of enzyme in excess of 500-fold over substrate concentrations to ensure single turnover conditions, and verified that the maximal rate of cleavage was observed in each kinetic experiment.

In addition, prior studies of DHT catalysis by EcoNth used substrate and enzyme concentrations well below K_d [12, 31]. Therefore, the binding component factored heavily into these observations, and the maximal catalytic rate was not observed. We ensured that our observations were made at enzyme concentrations both well above and well below K_d when possible, in order to accurately determine K_d . In some cases, (using the variant enzymes hNTHL1 Asp144Val and EcoNth Asp44Val (Table 3), the K_d is below the detection limits of our system, so the K_d reported is an upper limit, not the true K_d . Although EcoNth does not bind DHT:A as well as other substrates, this may not be an important factor in the cell. Cellular hNTHL1 concentrations are estimated to be greater than the apparent K_d (with the exception of substrate DHU:A with wild type hNTHL1), with values estimated from 2.3 μM in HeLa cell nuclei [19] to 25–80 nM in the nucleus of the mesothelial cell line LP9 [32]. From the yield of EcoNth during purification [33] and the reported cellular volume of *E. coli* [34], we can estimate that *E. coli* may have as much as 1.93 μM Nth, well above the K_d for DHT of 137 nM. The estimation of cellular enzyme concentrations cannot be made with much certainty, since the effects of macromolecular crowding and cellular compartmentalization are unknown. Nonetheless, it seems likely that hNTHL1 and EcoNth are both found in concentrations that saturate available substrate, and have similar substrate specificities as shown in Table 4.

Global determinants of Nth substrate specificity

We confirmed previous work showing hNTHL1 is slower than EcoNth [12, 35], and that both enzymes prefer lesions opposite G [15, 31]. Although we have shown that hNTHL1 is not catalytically faster than EcoNth when removing DHT, DHT is still removed by both enzymes more slowly than DHU (when compared paired to the same opposite base). A possible reason for the slower catalysis of DHT may be poor enzyme fit due to opposite base effects. The bulkier lesion thymine glycol is a better substrate than DHT [31], so lesion size alone cannot explain the difference.

Our initial goal was to identify specific amino acid(s) that controlled substrate recognition. However, we were unable to find a single determinant of substrate specificity either by statistically comparing about 150 Nth sequences, or by site-directed mutagenesis of likely amino acid residues. Because changes in the active site cavity of Nth produces only minor

alterations in substrate binding and catalysis, we propose that it is global, not point, contacts with DNA that determine substrate specificity. As further evidence, we superimposed EcoNth 2ABK over GstNth 1ORN in PYMOL [21], either by requiring alignment of the HhH motif, or alignment of the FeS cluster domain. When doing so, we could observe almost perfect alignment of the fixed domain, while the non-aligned domain no longer aligned well. Although clearly, enzymes from two different species were compared in this analysis, it is intriguing to consider that small conformational changes upon Nth binding to DNA may play a role in recognizing substrates.

Lesion recognition occurs prior to extrusion of the damage into the Nth active site

Recent crystallographic [36, 37], kinetics [10, 38] and single molecule studies [9, 11] provide strong evidence that DNA glycosylases locate damaged DNA bases by one-dimensional diffusion along the DNA helix that is random, bidirectional, and is consistent with tracking rotationally along the DNA backbone. The Nth glycosylases rely upon the insertion of three amino acids into the DNA helix to stabilize the duplex upon eversion of the damaged base into the enzyme's active site pocket and in EcoNth, these residues are Ile79, Leu81, and Gln41. A crystal structure of *G. stearothermophilus* Fpg glycosylase [36, 37] covalently bound to undamaged DNA showed that one of the three insertion residues of Fpg glycosylase is able to insert into the DNA base stack as a “wedge”, possibly to probe for damaged bases. When the corresponding “wedge residue” in EcoNth, Leu81, was substituted with an alanine, the Leu81Ala variant showed significantly reduced catalytic activity and single molecule analysis showed faster scanning on undamaged DNA than the wild-type Nth protein [11]. In addition, the Leu81Ala variant does not stop at damage as does the wild type EcoNth. Thus, *E. coli* Nth utilizes a wedge amino acid to intrahelically interrogate the DNA stack prior to base extrusion into the glycosylase active site. This mechanism provides an explanation for how the Nth search might be independent of specific interactions within the binding pocket, allowing for recognition of a diverse set of substrates. A recent stopped-flow kinetics analysis showed Nth to induce several fast sequential conformational changes in DNA during binding, lesion recognition and forming the catalytically competent structure and that the first phase of non-specific binding may be insertion of Leu81 [10]. Of note, the EcoNth Leu81 residue counterpart in hNTHL1 is Phe181, which is bulkier, and may “sense” aromatic structures. The wedge residue of hNTHL1 is followed by another bulky aromatic residue, tryptophan, whereas the prokaryotic wedge residue is followed by tyrosine.

In summary, the pair-wise design used allowed us to analyze opposite base effects separately from substrate effects, and to compare substrates differing only by a methyl group. We find, surprisingly, that the glycosylase specificity of the two enzymes is very similar. In addition, we've identified active site residues that contribute to substrate recognition but differ between the *E. coli* and human enzymes (Gln287 of hNTHL1 and Thr121 of EcoNth). Finally, we found that a key catalytic residue, Asp144 of hNTHL1, plays a different role than its corresponding residue in EcoNth. Thus, the kinetics studies described here have allowed us to further elucidate the basis for the substrate specificity of the Nth enzymes.

Acknowledgments

The authors thank Wendy Cooper (posthumously), Alicia Holmes and April Averill for preparing the enzymes used in this work.

Abbreviations

DHT	5,6-dihydrothymine
DHU	5,6-dihydrouracil
DTT	dithiothreitol
Tg	5,6-dihydro-5,6-dihydroxythymine (thymine glycol)
hNTHL1	human endonuclease III
EcoNth	<i>E. coli</i> endonuclease III

Bibliography

- Lindahl T, Barnes DE. Repair of endogenous DNA damage. *Cold Spring Harb Symp Quant Biol.* 2000; 65:127–133. [PubMed: 12760027]
- David SS, O'Shea VL, Kundu S. Base-excision repair of oxidative DNA damage. *Nature.* 2007; 447:941–950. [PubMed: 17581577]
- Duclos, S., Doublié, S., Wallace, SS. Consequences and Repair of Oxidative DNA Damage. In: Greim, H., Albertini, R.J., editors. *The Royal Society of Chemistry.* Cambridge, United Kingdom: 2012. p. 109-153.
- Kim YJ, Wilson DM 3rd. Overview of base excision repair biochemistry. *Current molecular pharmacology.* 2012; 5:3–13. [PubMed: 22122461]
- Prakash A, Doublié S, Wallace SS. The Fpg/Nei family of DNA glycosylases: substrates, structures, and search for damage. *Progress in molecular biology and translational science.* 2012; 110:71–91. [PubMed: 22749143]
- Wallace SS. DNA glycosylases search for and remove oxidized DNA bases. *Environ Mol Mutagen.* 2013; 54:691–704. [PubMed: 24123395]
- Wilson DM 3rd, Sofinowski TM, McNeill DR. Repair mechanisms for oxidative DNA damage. *Frontiers in bioscience: a journal and virtual library.* 2003; 8:d963–981. [PubMed: 12700077]
- Zharkov DO. Base excision DNA repair. *Cell Mol Life Sci.* 2008; 65:1544–1565. [PubMed: 18259689]
- Dunn AR, Kad NM, Nelson SR, Warshaw DM, Wallace SS. Single Qdot-labeled glycosylase molecules use a wedge amino acid to probe for lesions while scanning along DNA. *Nucleic Acids Res.* 2011; 39:7487–7498. [PubMed: 21666255]
- Kuznetsov NA, Kladova OA, Kuznetsova AA, Ishchenko AA, Saparbaev MK, Zharkov DO, Fedorova OS. Conformational Dynamics of DNA Repair by *Escherichia coli* Endonuclease III. *J Biol Chem.* 2015; 290:14338–14349. [PubMed: 25869130]
- Nelson SR, Dunn AR, Kathe SD, Warshaw DM, Wallace SS. Two glycosylase families diffusively scan DNA using a wedge residue to probe for and identify oxidatively damaged bases. *Proc Natl Acad Sci U S A.* 2014; 111:E2091–2099. [PubMed: 24799677]
- Katafuchi A, Nakano T, Masaoka A, Terato H, Iwai S, Hanaoka F, Ide H. Differential specificity of human and *Escherichia coli* endonuclease III and VIII homologues for oxidative base lesions. *J Biol Chem.* 2004; 279:14464–14471. [PubMed: 14734554]
- Ocampo-Hafalla MT, Altamirano A, Basu AK, Chan MK, Ocampo JE, Cummings A Jr, Boorstein RJ, Cunningham RP, Teebor GW. Repair of thymine glycol by hNth1 and hNeil1 is modulated by

- base pairing and cis-trans epimerization. *DNA Repair (Amst)*. 2006; 5:444–454. [PubMed: 16446124]
14. Miller H, Fernandes AS, Zaika E, McTigue MM, Torres MC, Wente M, Iden CR, Grollman AP. Stereoselective excision of thymine glycol from oxidatively damaged DNA. *Nucleic Acids Res*. 2004; 32:338–345. [PubMed: 14726482]
 15. Eide L, Luna L, Gustad EC, Henderson PT, Essigmann JM, Demple B, Seeberg E. Human endonuclease III acts preferentially on DNA damage opposite guanine residues in DNA. *Biochemistry*. 2001; 40:6653–6659. [PubMed: 11380260]
 16. Ocampo MT, Chung W, Marenstein DR, Chan MK, Altamirano A, Basu AK, Boorstein RJ, Cunningham RP, Teebor GW. Targeted deletion of mNth1 reveals a novel DNA repair enzyme activity. *Mol Cell Biol*. 2002; 22:6111–6121. [PubMed: 12167705]
 17. Marenstein DR, Ocampo MT, Chan MK, Altamirano A, Basu AK, Boorstein RJ, Cunningham RP, Teebor GW. Stimulation of human endonuclease III by Y box-binding protein 1 (DNA-binding protein B). Interaction between a base excision repair enzyme and a transcription factor. *J Biol Chem*. 2001; 276:21242–21249. [PubMed: 11287425]
 18. Venkhataraman R, Donald CD, Roy R, You HJ, Doetsch PW, Kow YW. Enzymatic processing of DNA containing tandem dihydrouracil by endonucleases III and VIII. *Nucleic Acids Res*. 2001; 29:407–414. [PubMed: 11139610]
 19. Liu X, Choudhury S, Roy R. *In vitro* and *in vivo* dimerization of human endonuclease III stimulates its activity. *J Biol Chem*. 2003; 278:50061–50069. [PubMed: 14522981]
 20. Fromme JC, Verdine GL. Structure of a trapped endonuclease III-DNA covalent intermediate. *EMBO J*. 2003; 22:3461–3471. [PubMed: 12840008]
 21. DeLano, WL. The PyMOL Molecular Graphics System. DeLano Scientific; Palo Alto, CA: 2002.
 22. Thayer MM, Ahern H, Xing D, Cunningham RP, Tainer JA. Novel DNA binding motifs in the DNA repair enzyme endonuclease III crystal structure. *EMBO J*. 1995; 14:4108–4120. [PubMed: 7664751]
 23. Faucher F, Robey-Bond SM, Wallace SS, Doublet S. Structural characterization of *Clostridium acetobutylicum* 8-oxoguanine DNA glycosylase in its apo form and in complex with 8-oxodeoxyguanosine. *J Mol Biol*. 2009; 387:669–679. [PubMed: 19361427]
 24. Gu X. Maximum-likelihood approach for gene family evolution under functional divergence. *Mol Biol Evol*. 2001; 18:453–464. [PubMed: 11264396]
 25. Watanabe T, Blaisdell JO, Wallace SS, Bond JP. Engineering functional changes in *Escherichia coli* endonuclease III based on phylogenetic and structural analyses. *J Biol Chem*. 2005; 280:34378–34384. [PubMed: 16096281]
 26. Studier FW. Protein production by auto-induction in high density shaking cultures. *Protein Expr Purif*. 2005; 41:207–234. [PubMed: 15915565]
 27. Bandaru V, Blaisdell JO, Wallace SS. Oxidative DNA glycosylases: recipes from cloning to characterization. *Methods Enzymol*. 2006; 408:15–33. [PubMed: 16793360]
 28. Blaisdell JO, Wallace SS. Rapid determination of the active fraction of DNA repair glycosylases: a novel fluorescence assay for trapped intermediates. *Nucleic Acids Res*. 2007; 35:1601–1611. [PubMed: 17289752]
 29. Liu X, Roy R. Truncation of amino-terminal tail stimulates activity of human endonuclease III (hNTH1). *J Mol Biol*. 2002; 321:265–276. [PubMed: 12144783]
 30. Porello SL, Leyes AE, David SS. Single-turnover and pre-steady-state kinetics of the reaction of the adenine glycosylase MutY with mismatch-containing DNA substrates. *Biochemistry*. 1998; 37:14756–14764. [PubMed: 9778350]
 31. Asagoshi K, Odawara H, Nakano H, Miyano T, Terato H, Ohyama Y, Seki S, Ide H. Comparison of substrate specificities of *Escherichia coli* endonuclease III and its mouse homologue (mNTH1) using defined oligonucleotide substrates. *Biochemistry*. 2000; 39:11389–11398. [PubMed: 10985784]
 32. Odell ID, Newick K, Heintz NH, Wallace SS, Pederson DS. Non-specific DNA binding interferes with the efficient excision of oxidative lesions from chromatin by the human DNA glycosylase, NEIL1. *DNA Repair (Amst)*. 2010; 9:134–143. [PubMed: 20005182]

33. Asahara H, Wistort PM, Bank JF, Bakerian RH, Cunningham RP. Purification and characterization of *Escherichia coli* endonuclease III from the cloned nth gene. *Biochemistry*. 1989; 28:4444–4449. [PubMed: 2669955]
34. Kubitschek HE. Cell volume increase in *Escherichia coli* after shifts to richer media. *J Bacteriol*. 1990; 172:94–101. [PubMed: 2403552]
35. Ikeda S, Biswas T, Roy R, Izumi T, Boldogh I, Kurosky A, Sarker AH, Seki S, Mitra S. Purification, characterization of human NTH1, a homolog of *Escherichia coli* endonuclease III. Direct identification of Lys-212 as the active nucleophilic residue. *J Biol Chem*. 1998; 273:21585–21593. [PubMed: 9705289]
36. Banerjee A, Santos WL, Verdine GL. Structure of a DNA glycosylase searching for lesions. *Science*. 2006; 311:1153–1157. [PubMed: 16497933]
37. Qi Y, Nam K, Spong MC, Banerjee A, Sung RJ, Zhang M, Karplus M, Verdine GL. Strandwise translocation of a DNA glycosylase on undamaged DNA. *Proc Natl Acad Sci U S A*. 2012; 109:1086–1091. [PubMed: 22219368]
38. Kuznetsov NA, Bergonzo C, Campbell AJ, Li H, Mechetin GV, de los Santos C, Grollman AP, Fedorova OS, Zharkov DO, Simmerling C. Active destabilization of base pairs by a DNA glycosylase wedge initiates damage recognition. *Nucleic Acids Res*. 2015; 43:272–281. [PubMed: 25520195]

Highlights

- *E. coli* Asp44 plays a different role than its homologous residue in human NTHL1
- hNTHL1 Gln287 is involved in opposite base specificity as well as catalysis
- EcoNth Thr121 is involved in DNA binding and catalysis
- EcoNth and hNTHL1 demonstrate similar substrate specificity for DHT

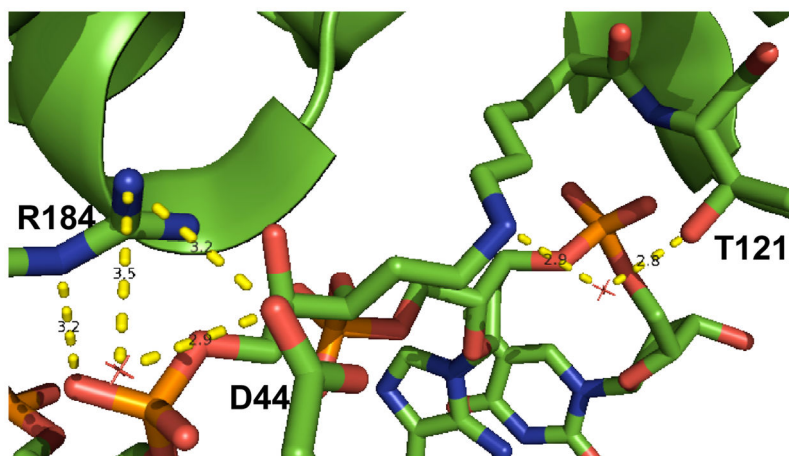


Figure 1. Pymol rendering of GstNth (1ORN) with variants described in this paper highlighted. Numbering is according to EcoNth. Hydrogen bonding is indicated by yellow dashes. Note Thr121 shares a water molecule with the Schiff base (DNA to K120). Asp44 and Arg184 also co-position with a water molecule, and Arg184 stabilizes the 3' phosphate of the lesion.

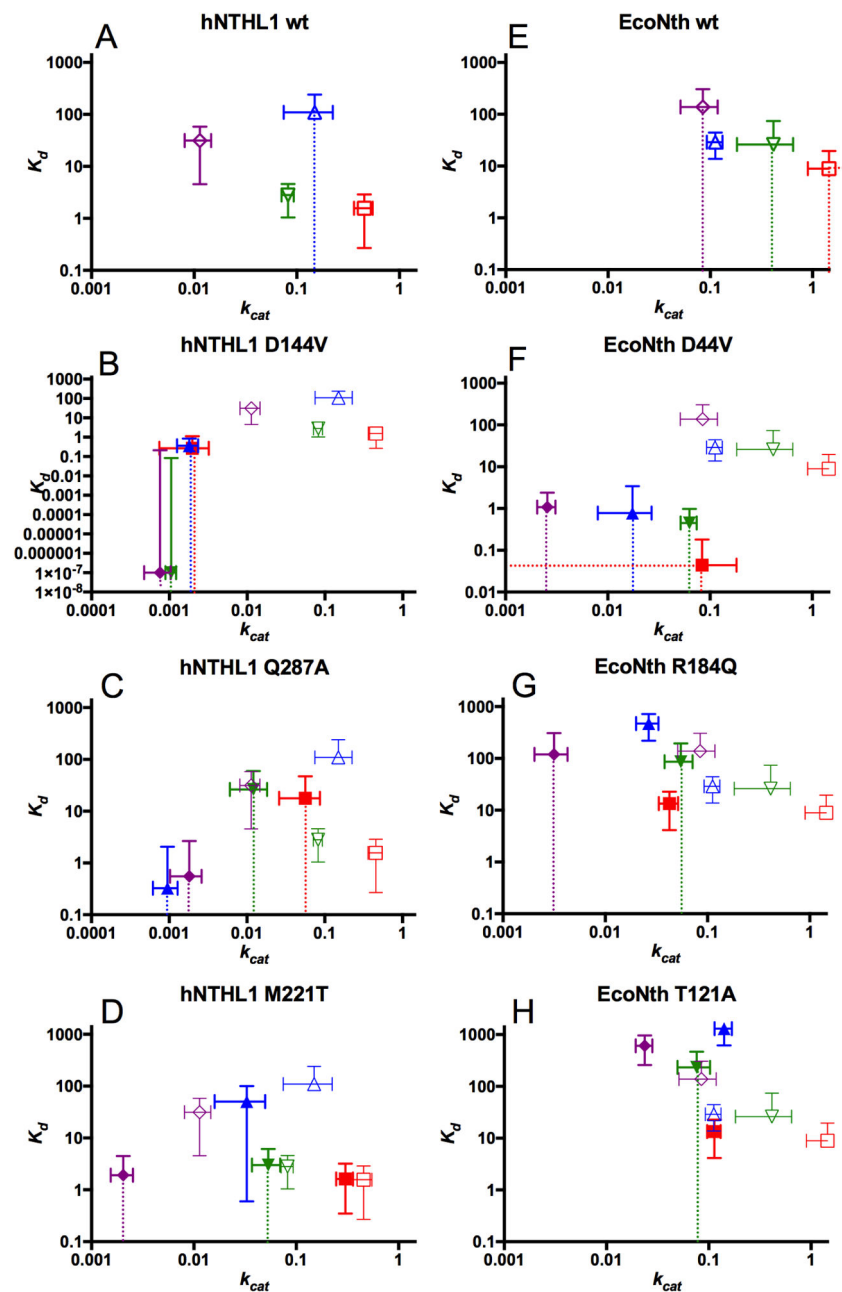


Figure 2.

k_{cat} versus K_d graphs for hNTHL1 and EcoNth wild type enzymes, and three variants of each enzyme. k_{cat} is plotted versus K_d for each enzyme and variant, and for each substrate. Each graph is labeled with the enzyme name. A, hNTHL1 wild type. B, hNTHL1 Asp144Val. C, hNTHL1 Gln287Ala. D, hNTHL1 Met221Thr. E, EcoNth wild type. F, EcoNth Asp44Val. G, EcoNth Arg184Gln. H, EcoNth Thr121Ala. DHU:G is shown in red, DHU:A in blue, DHT:G in green and DHT:A in purple. For reference, the wild type values are shown on the variant graphs in pastel outlines rather than filled full color. Error bars

show the 95% confidence intervals. Dotted error bars indicate there is no bound on the limit.
Note the log scale axis.

Author Manuscript

Author Manuscript

Author Manuscript

Author Manuscript

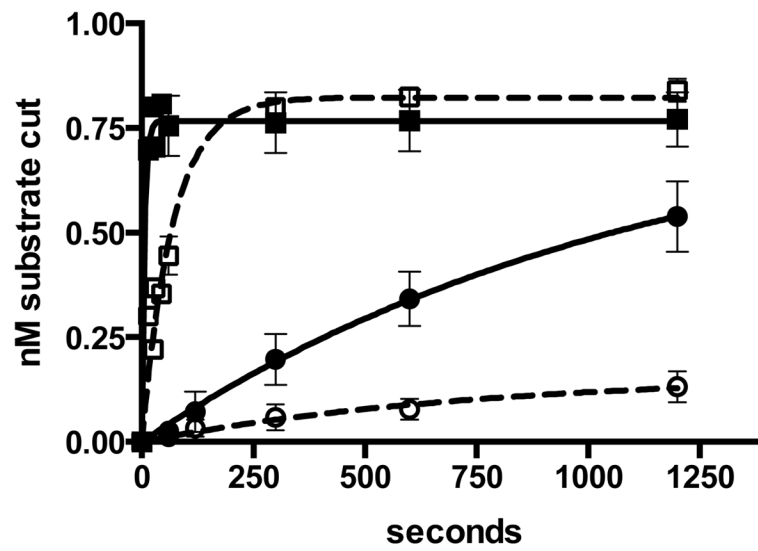
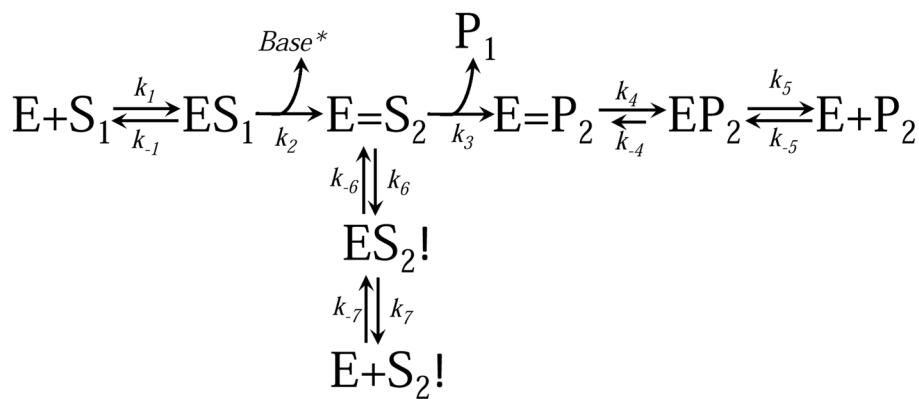


Figure 3. Time course of hNTHL1 Asp144Val (circles) glycosylase (closed) and bifunctional (open) activity compared with wildtype hNTHL1 (squares). Enzyme concentration = 10 nM, DHU:G concentration = 1 nM.



Scheme 1.

(Modified from [17]). E represents enzyme, S₁ represents double-stranded DNA oligonucleotide (substrate) with an oxidatively damaged nucleotide, *Base* represents the cleaved oxidized base, S₂ represents the substrate with an AP site, P₁ is the leaving end of substrate with nicked backbone (3' β-eliminated), and P₂ is the 5' end of the substrate after β-elimination. The Schiff base between enzyme and substrate is depicted with a double bond. *k*₁ and *k*₋₁ are the rates of substrate association and dissociation from enzyme, respectively. *k*₂ is the rate of base release, *k*₃ is the rate of β-elimination, *k*₄ and *k*₋₄ are the forward and reverse rates of Schiff base hydrolysis, *k*₅ and *k*₋₅ are the forward and reverse rates of produce release from or re-association with enzyme. Enzymatic resolution of the Schiff base may occur with the rates *k*₆ and *k*₋₆, and release of AP substrate with the rates *k*₇ and *k*₋₇.

Table 1

hNTHL1 and EcoNth variants studied. Initial screening was performed for these 20 variants. Of these, six were chosen for complete kinetic analysis (*in italics*).

hNTHL1	EcoNth
	Thr22Ala
Ser139Val	Val36Thr
Ser140Ala	Ala40Ser
<i>Asp144Val</i>	<i>Asp44Val</i>
<i>Met221Thr</i>	Thr121Met, <i>Thr121Ala</i>
Ala227Asn	Asn127Ala, Asn127Gly
Asn279His	His176Asn
Gly280His	His177Gly
Gln287Arg, <i>Gln287Ala</i>	<i>Arg184Gln</i>

Author Manuscript

Author Manuscript

Author Manuscript

Author Manuscript

Table 2

k_{cat} (per second)

hNTHL1 and EcoNth wild type and variant enzymes. The substrate concentration was 2 nM or less, and enzyme concentrations varied from 5–1000 nM, depending on the enzyme and substrate combination. Substrates in italics are cognate base pairs. 95% confidence intervals shown under “confidence”.

Substrate	hNTHL1	k _{cat}	confidence	EcoNth	k _{cat}	confidence
DHU:G	Wild type	0.45	0.36 – 0.55	Wild type	1.45	0.90 – 2.00
DHU:A	Wild type	0.15	0.07 – 0.22	Wild type	0.11	0.09 – 0.13
DHT:G	Wild type	0.08	0.07 – 0.09	Wild type	0.41	0.18 – 0.65
DHT:A	Wild type	0.01	0.008 – 0.014	Wild type	0.08	0.05 – 0.12
DHU:G	Asp144Val	0.0020	0.0007 – 0.0032	Asp44Val	0.084	0.072 – 0.182
DHU:A	Asp144Val	0.0018	0.0013 – 0.0023	Asp44Val	0.017	0.008 – 0.027
DHT:G	Asp144Val	0.0011	0.0009 – 0.0011	Asp44Val	0.063	0.052 – 0.074
DHT:A	Asp144Val	0.0008	0.0005 – 0.0010	Asp44Val	0.003	0.0020 – 0.0031
DHU:G	Gln287Ala	0.056	0.026 – 0.087	Arg184Gln	0.043	0.033 – 0.052
DHU:A	Gln287Ala	0.001	0.0006 – 0.0013	Arg184Gln	0.027	0.020 – 0.033
DHT:G	Gln287Ala	0.012	0.006 – 0.018	Arg184Gln	0.055	0.038 – 0.071
DHT:A	Gln287Ala	0.002	0.0010 – 0.003	Arg184Gln	0.003	0.002 – 0.004
DHU:G	Met221Thr	0.302	0.246 – 0.359	Thr121Ala	0.114	0.097 – 0.131
DHU:A	Met221Thr	0.033	0.016 – 0.050	Thr121Ala	0.141	0.114 – 0.169
DHT:G	Met221Thr	0.053	0.037 – 0.070	Thr121Ala	0.076	0.050 – 0.103
DHT:A	Met221Thr	0.002	0.0015 – 0.0025	Thr121Ala	0.024	0.019 – 0.028

Table 3

K_d (nM)

hNTHL1 and EcoNth wild type and variant enzymes. The substrate concentration was 2 nM or less, and enzyme concentrations varied from 5–1000 nM, depending on the enzyme and substrate combination. Substrates in italics are cognate base pairs. 95% confidence intervals shown under “confidence”.

Substrate	hNTHL1	K _d	confidence	EcoNth	K _d	confidence
DHU:G	Wild type	1.57	0.26 – 2.87	Wild type	8.95	0.0 – 19.64
DHU:A	Wild type	109	0.00 – 241	Wild type	29.0	13.8 – 44.3
DHT:G	Wild type	2.81	1.04 – 4.58	Wild type	26.0	0.0 – 73.8
DHT:A	Wild type	31.3	4.54 – 58.1	Wild type	138	0.0 – 305
DHU:G	Asp144Val	0.269	0 – 1.12	Asp44Val	0.044	0.0 – 0.182
DHU:A	Asp144Val	0.359	0 – 0.851	Asp44Val	0.779	0.0 – 3.41
DHT:G	Asp144Val	1×10 ⁻⁷	0 – 0.084	Asp44Val	0.450	0.0 – 0.976
DHT:A	Asp144Val	1×10 ⁻⁷	0 – 0.21	Asp44Val	1.08	0.0 – 2.39
DHU:G	Gln287Ala	17.7	0.0 – 47.2	Arg184Gln	13.4	4.12 – 22.8
DHU:A	Gln287Ala	0.33	0.0 – 2.06	Arg184Gln	471	221 – 721
DHT:G	Gln287Ala	26.4	0.0 – 59.8	Arg184Gln	86.1	0.0 – 195
DHT:A	Gln287Ala	0.55	0.0 – 2.66	Arg184Gln	120	0.0 – 308
DHU:G	Met221Thr	1.62	0.35 – 2.89	Thr121Ala	32.5	9.55 – 55.4
DHU:A	Met221Thr	50.4	0.590 – 100	Thr121Ala	1310	621 – 1990
DHT:G	Met221Thr	3.00	0.0 – 6.12	Thr121Ala	233	0.0 – 512
DHT:A	Met221Thr	1.92	0.0 – 4.48	Thr121Ala	610	259 – 961

Table 4

Enzyme-substrate specificity k_{cat}/K_d

Substrate	hNTHL1	k_{cat}/K_d	EcoNth	k_{cat}/K_d
DHU:G	Wild type	0.290	Wild type	0.162
DHU:A	Wild type	0.001	Wild type	0.004
DHT:G	Wild type	0.029	Wild type	0.016
DHT:A	Wild type	0.0004	Wild type	0.0006
DHU:G	Asp144Val	0.0074	Asp44Val	1.900
DHU:A	Asp144Val	0.0050	Asp44Val	0.022
DHT:G	Asp144Val	10500	Asp44Val	0.140
DHT:A	Asp144Val	7590	Asp44Val	0.002
DHU:G	Gln287Ala	0.00318	Arg184Gln	0.0031
DHU:A	Gln287Ala	0.00290	Arg184Gln	5.64E-05
DHT:G	Gln287Ala	0.00046	Arg184Gln	0.0006
DHT:A	Gln287Ala	0.00328	Arg184Gln	2.63E-05
DHU:G	Met221Thr	0.187	Thr121Ala	0.0034
DHU:A	Met221Thr	0.001	Thr121Ala	0.0001
DHT:G	Met221Thr	0.018	Thr121Ala	0.0003
DHT:A	Met221Thr	0.001	Thr121Ala	3.881E-05